GEOPHYSICAL RESEARCH LETTERS, VOL. 34, L18305, doi:10.1029/2007GL031162, 2007

Magnetostratigraphy of an early-middle Miocene loess-soil sequence in the western Loess Plateau of China

Qingzhen Hao[1] and Zhengtang Guo[1]

Received 3 July 2007; revised 21 August 2007; accepted 24 August 2007; published 25 September 2007.

[1] Stratigraphy and magnetic susceptibility of the Quaternary eolian deposits at different sites in China can be closely correlated, confirming their spatial coherence and temporal continuity. The extent to which these conclusions are true for the Miocene loess-soil sequences remains to be addressed. Here, a 231.9-m eolian section, QA-III, is geomagnetically dated, yielding an age span of 21.4–11.4 Ma, with the portion older than 19.6 Ma being partially water-reworked. The magnetozones, lithologic structure and magnetic susceptibility of the sequence are highly correlative with the QA-I and QA-II sections, 30 km west of QA-III. These sequences demonstrate that the Miocene loess deposits are also spatially correlative in stratigraphy, present a near-continuous sequence of paleoenvironment changes, and that magnetic susceptibility is a useful tool for stratigraphic correlation. The basal age of QA-III confirms again the onset of Asian inland deserts and monsoon-dominate climates by the early Miocene. **Citation:** Hao, Q., and Z. Guo (2007), Magnetostratigraphy of an early-middle Miocene loess-soil sequence in the western Loess Plateau of China, *Geophys. Res. Lett.*, *34*, L18305, doi:10.1029/2007GL031162.

1. Introduction

[2] The reported Miocene loess-soil sequences at Qinan County in the western Loess Plateau provide an important terrestrial eolian record of paleoclimate [*Guo et al.*, 2002]. They consist of alternating reddish soils and yellow-brown or brown loess horizons, similar to the Quaternary loess-soil sequences in northern China. Their morphological features, mineral assemblage, grain shapes, grain-size distribution and geochemical components are characteristic of eolian dust deposits [*Guo et al.*, 2002]. Their eolian origin was further confirmed by detailed sedimentological and malacological studies [*Liu et al.*, 2006; *Li et al.*, 2006; *Qiao et al.*, 2006].

[3] The reported QA-I (22–6.2 Ma) and QA-II (21.6–7.4 Ma, 2 km northeast to QA-I) sections [*Guo et al.*, 2002] placed the onset of eolian deposition at least fourteen million years earlier than previously recognized based on the *Red-Clay* [*Ding et al.*, 1998; *An et al.*, 2001; *Guo et al.*, 2001]. Their Miocene ages are also confirmed by micro-mammalian fossil assemblages [*Guo et al.*, 2002]. Recently, eolian deposits of middle-late Miocene ages were also reported from the high terraces near Xining [*Lu et al.*, 2004]. The onset of eolian deposition in northern China indicates that large source areas of eolian dust in the interior of Asia and energetic winter monsoon winds as dust carrier must have existed by 22 Ma BP, while the alternations between loess and soil layers indicate cyclical changes in the summer and winter monsoons [*Guo et al.*, 2002].

[4] The stratigraphy [*Liu*, 1985; *Kukla and An*, 1989] and climate proxies [e.g., *Guo et al.*, 2000] of the Quaternary loess-soil sequences in northern China have been shown to be spatially correlative. Magnetic susceptibility can be used for stratigraphic [*Kukla and An*, 1989] and climatic [*Sun et al.*, 1996; *Hao and Guo*, 2005] correlations. The extent to which these conclusions are true for the Miocene loess-soil sequences remains to be addressed. For this purpose, establishment of new sequences at remoter sites is essential. This is also helpful for spatial studies of paleoclimate.

[5] In this paper, we present magnetostratigraphic results for a new Miocene loess section (QA-III) in the western Loess Plateau (Figure 1). We show also that the field lithology structure, magnetostratigraphy, and magnetic susceptibility records of these sequences are spatially coherent and that magnetic susceptibility is a good tool for stratigraphy correlation of the Miocene eolian deposits in China.

2. Geological Settings and Methods

[6] The new QA-III section (105°48′E, 35°01′N) is situated about 30 km east to the QA-I section and about 5 km north of the late Miocene-Pliocene Dongwan (DW) loess-soil sequence [*Hao and Guo*, 2004] (Figure 1). The section is exposed in the gullies at the sides of a SSW-NNE trending hill and is composed of two natural outcrops. The connection of the two outcrops was firstly established using field stratigraphic markers and then confirmed by magnetostratigraphy and magnetic susceptibility records of a 32.4 m overlapping portion. The sections rest on metamorphic bedrocks of early Sinian age (680–543 Ma) and are uncomfortably overlain by late Quaternary loess, 10–30 m thick.

[7] The total thickness of the QA-III section is 231.9 m. The upper 180.2 m consists of alternating loess and soil layers, and the lower-most portion contains some fine stratifications resulted from sheet-flow processes due to undulated paleotopography, but still with interbedded soils (Figure 2). Some bedrock fragments (<1 cm) are observed in some soil layers below 221.1 m. Quartz grains up to 1–2 mm in diameter were also noted within a few layers at the lower part of the outcrops, but in scarce abundance. They are attributable to local wind deflation from the bedrock of the nearby highlands.

[8] 2672 samples were taken at 10 cm interval for magnetic susceptibility measurements and 1100 oriented samples were taken at about 25 cm intervals for magneto-

[1]Institute of Geology and Geophysics, Chinese Academy of Sciences, Beijing, China.

0094-8276/07/2007GL031162$05.00

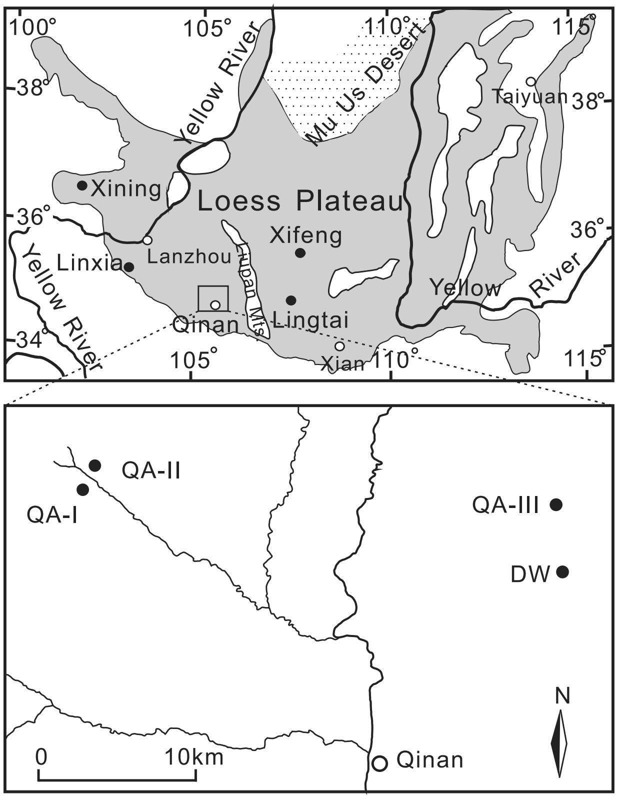

Figure 1. Map showing the Loess Plateau in northern China and the locations of the sites discussed.

stratigraphic study. Block samples were cut into 2 cm cubes, demagnetized in a MMTD600 thermal demagnetizer and measured with a 2G three-axis cryogenic magnetometer (Paleomagnetism Laboratory of the IGGCAS). The instruments were housed in a magnetically shielded room to avoid contamination by viscous magnetization. Magnetic susceptibility was measured on air-dried samples using a Bartington MS2 unit.

[9] We performed stepwise thermal demagnetizations on 56 pilot samples at ~5 m intervals up to a temperature of 680°C. Typical demagnetization diagrams for normal and revered samples are shown in Figure 3. Secondary viscous magnetization parallel to the present-day field or acquired during storage was removed by heating to 300°C, occasionally 400°C. A characteristic remanent magnetization (ChRM) of either normal or reversed polarity was typically isolated above these temperatures. To improve the efficiency, the other samples were demagnetized in 6–10 steps from 250 or 300°C using increments of 30 or 50°C.

3. Results and Discussion

[10] The magnetostratigraphy of the QA-III section is shown in Figure 2. Virtual geomagnetic pole (VGP) latitudes of the ChRM component, calculated by means of principal component analysis [*Kirschvink*, 1980], were used to establish the magnetozones. The sequences show 20 normal and 21 reversed magnetozones.

[11] The magnetozones can be unambiguously calibrated to the GPTS of CK95 [*Cande and Kent*, 1995]. Between the 0 and 18.1 m, the two thick reversal magnetozones interbedded with a thin normal magnetozone are correlated to Chrons C5r.2r to C5r.3r. The interval of 18.1–30.4 m consists of two normal magnetozones interbedded with a small reversal one and is correlative with Chron C5An. The reversal Chron C5Ar is located between 30.4 and 42.0 m, containing two small normal polarity zones. Consequently, the six continuous normal magnetozones between 42.0 to 100.9 m are correlative to Chrons C5AAn, C5ABn, C5ACn, C5ADn, C5Bn.1n, and C5Bn.2n, respectively.

[12] The interval 100.9–142.6 m contains two longer reversal magnetozones interbedded with three closely spaced short normal ones, evidently corresponds to the zonation from Chrons C5Br to C5Cr in the GPTS [*Cande and Kent*, 1995]. The followed magnetozone between 142.6 and 146.7 m matches Chron C5Dn. The short normal magnetozone between 153.8 and 155.3 m appears to be correlative with Cryptochron C5Dr-1. Below 161.6 m, the four normal magnetozones are assigned to Chrons C5En, C6n, C6An.1n, C6An.2n, respectively. The section ends in the reversal magnetozone of C6Ar.

[13] The magnetostratigraphy of QA-III therefore defines a near-continuous sequence from Chron C6Ar to Chron C5r.2r. Extrapolations based on sedimentation rate suggest the basal and top ages of 21.38 and 11.35 Ma BP, respectively. The boundary between the upper typical loess-soil sequence and lower water-reworked loess is dated at 19.6 Ma.

[14] The magnetozone sequences and magnetic susceptibility of the new section are highly correlative with those of the QA-I and QA-II sections. Their long-term changes of magnetic susceptibility are closely similar, characterized by higher values from 14.4 Ma to 16.3 Ma, lower values above and below this interval (Figure 4). In QA-III, the higher sedimentation rate prior to Chron C6r is attributable to sheet-flow processes. Because the section is 30 km far from the QA-I site, the above results demonstrate that the Miocene loess deposits in western Loess Plateau are spatially correlative and have a near-continuous nature at the scale of magnetozones.

[15] Magnetic susceptibility is widely used for stratigraphy correlations in Quaternary loess [e.g., *Kukla and An*, 1989] and in the late Neogene *Red Earth Formation* [e.g., *Guo et al.*, 2001]. Our study demonstrates that magnetic susceptibility can also be used as a reliable and rapid tool for stratigraphy correlation of the Miocene loess-soil sequences. As in the Quaternary sequences [e.g., *Zhou et al.*, 1990; *Heller et al.*, 1993], magnetic susceptibility is higher in soils than in the surrounding loess and this is attributable to pedogenesis. Our preliminary rock magnetic study suggests enriched superparamagnetic magnetite/maghemite in the 80–123.05 m interval that would be responsible to the higher susceptibility values. Detailed rock magnetic results will be reported elsewhere.

[16] The lithology of QA-III can be visually structured into six major intervals and these allow close comparison with QA-I and QA-II. The interval 0–48.0 m contains stronger soils with visually observable clay illuvial features, and is comparable to the 59.8–99.9 m interval in QA-I with

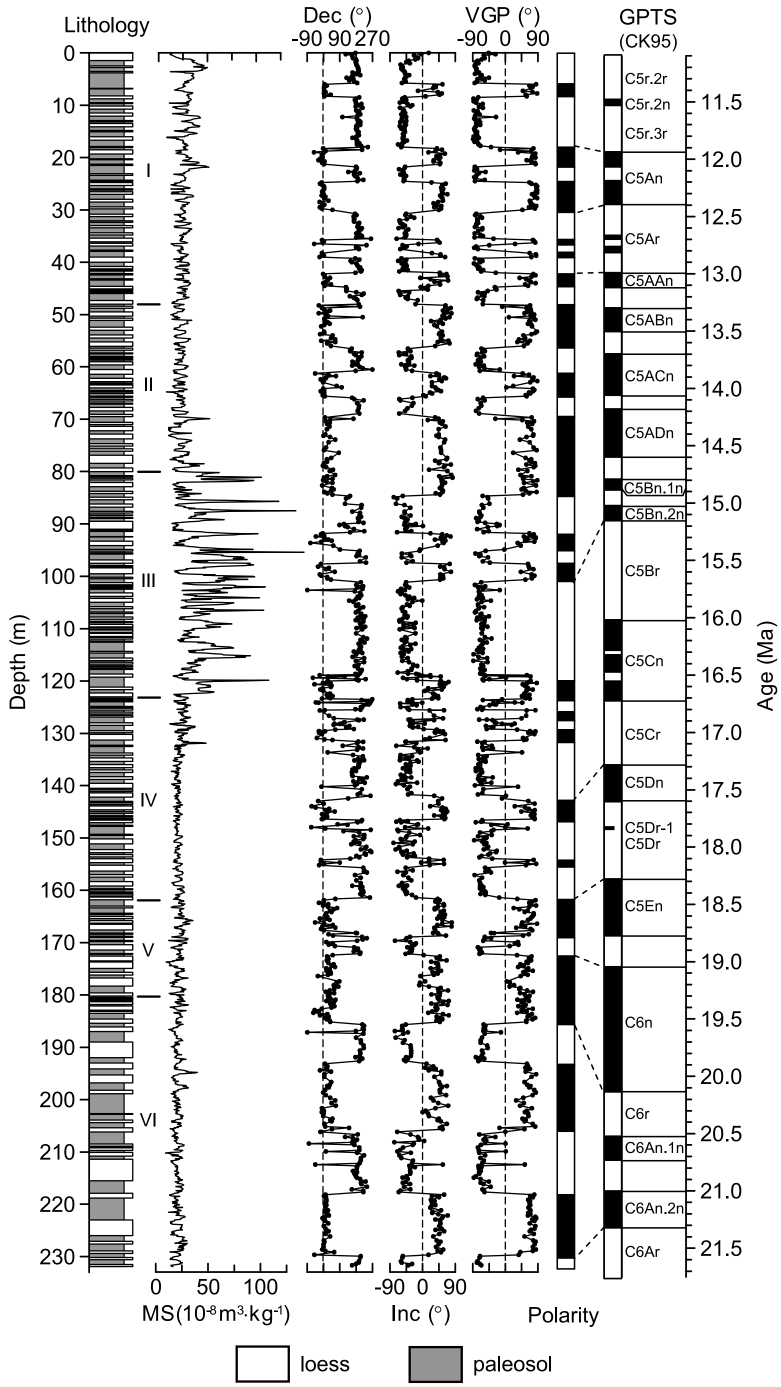

Figure 2. Lithology, magnetic susceptibility (MS) and magnetostratigraphy of the QA-III loess-soil section. Black bars indicate normal polarity and white bars indicate reversed polarity. Note the interval from 180.2 m to 231.9 m contains some sheet-flow affected features and bedrock fragments.

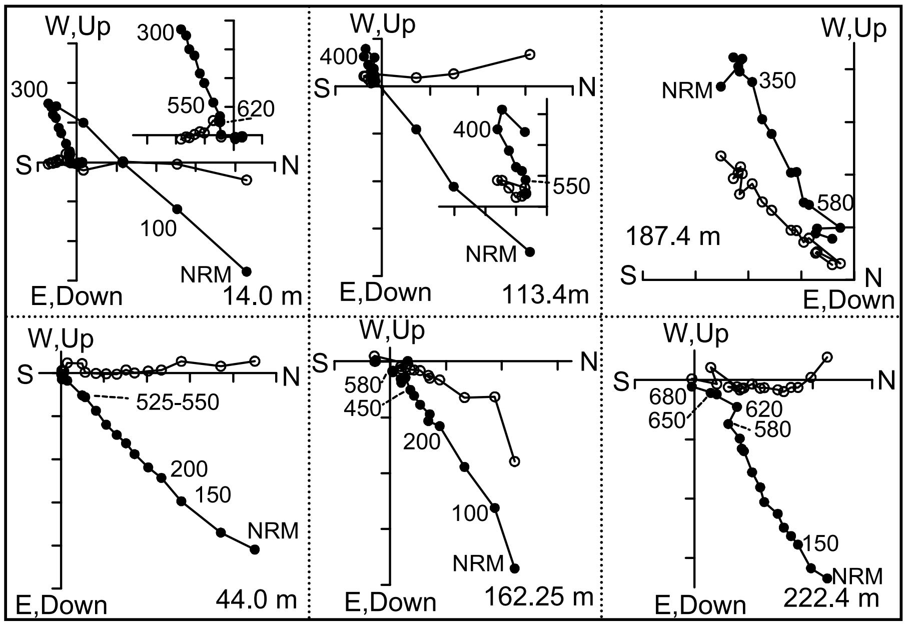

Figure 3. Orthogonal projections of representative progressive thermal demagnetization experiments. The open (solid) circles refer to the horizontal (vertical) plane.

similar age. The soils within the 48.0–80.0 m interval are less developed with less illuvial features and are similar to the soils within the 99.9–128.6 m interval in QA-I. The 80.0–123.05 m interval contains again more strongly developed soils. Similar soils are observed in the corresponding 128.6–166.0 m interval of QA-I. Weak soils are observed in the 123.05–161.8 m interval at QA-III and in the 166.0–200.0 m interval of QA-I that have similar ages. The most strongly developed soils are observed in the 161.8 to 180.2 m interval of QA-III, fully consistent with the early Miocene portion at QA-I. Although sediments spanning the 180.2–231.9 m interval in QA-III are partially water-reworked, the strongly developed soils are similar to the lower-most part in QA-I.

[17] This new section, combined with QA-I and QA-II [*Guo et al.*, 2002] also indicates the wide distribution of the Miocene loess deposits. Portions of eolian deposits of Miocene age have also been reported near Xining [*Lu et al.*, 2004]. The fine materials in the Linxia lacustrine basin (Figure 1) are also isotopically identified as derived from eolian dust [*Garzione et al.*, 2005].

[18] Loess deposits require sizable source areas arid enough to create eolian dust, and an atmospheric circulation sufficiently energetic to carry dust particles. The high degree of similarity in geochemical properties between the Miocene loess and the Quaternary loess suggests rather similar dust source areas and a comparable dust transporting trajectory [*Guo et al.*, 2002]. Quaternary loess deposits in northern China mainly came from the desert lands to the north and northwest [*Liu*, 1985]. The widespread and near-continuous nature of the Miocene loess in the western Loess Plateau indicates that the sizable deserts must have existed in the interior of Asia by the early Miocene times and have been maintained from that time to the present day. This is consistent with the increased Asian eolian inputs to the North Pacific at ~20 Ma [*Rea*, 1994; *Ziegler et al.*, 2007].

[19] The alternations between loess and reddish soils in the Miocene eolian deposits indicate cyclical changes in the strength of the winter and summer monsoon, because strong soils need a summer circulation bringing moisture while dust transport requires quite different circulation. These two circulations systems must alternate seasonally with contrasted trajectories. Thus, the early Miocene basal age of these loess-soil sequences provide robust evidence for the onset of the monsoon climate in northern China. Up to now, the basal age of 22 Ma BP of QA-I section represents the oldest in northern China, indicating a reorganization of the climate system around the Miocene/Oligocene boundary in East Asia. This is consistent with the results obtained from spatial examinations of climate indicators [*Liu and Guo*, 1997; *Sun and Wang*, 2005].

4. Conclusion

[20] This study has dated a new Miocene section by magnetostratigraphic methods and the magnetic polarity zonation correlates well with the portion of Chron C6Ar to C5r.2r in the GPTS [*Cande and Kent*, 1995]. The new section consists of two parts: the typical loess-soil sequence (11.4–19.6 Ma BP) and the water-reworked loess (19.6–21.4 Ma BP). The lithology structure, magnetostratigraphy, and magnetic susceptibility of QA-III younger than 19.6 Ma BP correlate well with the previously published QA-I and QA-II sections. These sequences demonstrate that the Miocene loess in the western Loess Plateau is a near-continuous paleoenvironmental record, and that magnetic susceptibility can be used as a tool for stratigraphic correlation. The ages of the three reported sequences (QA-I, QA-II, QA-III) also

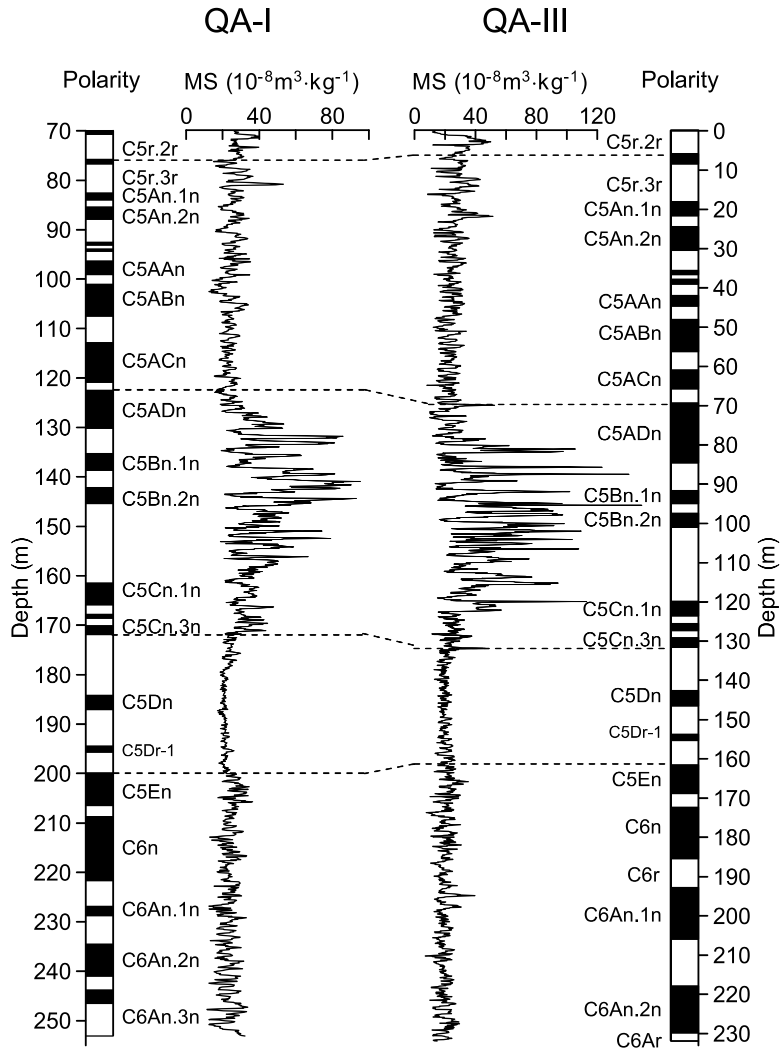

Figure 4. Correlation of magnetic susceptibility (MS) and paleomagnetic polarity records between QA-III and QA-I sections.

confirm the onset of Asian inland desertification and monsoon climate in northern China by the early Miocene.

[21] **Acknowledgments.** This study is supported by the Chinese Academy of Sciences (KZCX3-SW-139), 973 Project 2004CB720203, and the National Natural Science Foundation of China (40672115). We are grateful to Stefanie Brachfeld and an anonymous reviewer for the helpful comments and suggestions. Thanks are extended to R. X. Zhu for helpful discussions and to Y. S. Qiao, S. Z. Peng, J. F. Liu, J. J Wei and Z. S. Zhang for field and/or laboratory assistance.

References

An, Z. S., J. E. Kutzbach, W. L. Prell, and S. C. Porter (2001), Evolution of Asian monsoons and phased uplift of the Himalaya-Tibetan Plateau since late Miocene time, *Nature*, *411*, 62–66.

Cande, S. C., and D. V. Kent (1995), Revised calibration of the geomagnetic polarity timescale for the Late Cretaceous and Cenozoic, *J. Geophys. Res.*, *100*, 6093–6095.

Ding, Z. L., J. M. Sun, S. L. Yang, and T. S. Liu (1998), Preliminary magnetostratigraphy of a thick eolian red clay-loess sequence at Lingtai, the Chinese Loess Plateau, *Geophys. Res. Lett.*, *25*, 1225–1228.

Garzione, C. N., M. J. Ikari, and A. R. Basu (2005), Source of Oligocene to Pliocene sedimentary rocks in the Linxia Basin in northeastern Tibet from Nd isotopes: Implications for tectonic forcing of climate, *GSA Bull.*, *117*, 1156–1166.

Guo, Z. T., P. Biscaye, L. Y. Wei, X. H. Chen, S. Z. Peng, and T. S. Liu (2000), Summer monsoon variations over the last 1.2 Ma from the weathering of loess-soil sequences in China, *Geophys. Res. Lett.*, *27*, 1751–1754.

Guo, Z. T., S. Z. Peng, Q. Z. Hao, P. E. Biscaye, and T. S. Liu (2001), Origin of the Miocene-Pliocene Red-Earth Formation at Xifeng in northern China and implications for paleoenvironments, *Palaeogeogr. Palaeoclimatol. Palaeoecol.*, *170*, 11–26.

Guo, Z. T., W. F. Ruddiman, Q. Z. Hao, H. B. Wu, Y. S. Qiao, R. X. Zhu, S. Z. Peng, J. J. Wei, B. Y. Yuan, and T. S. Liu (2002), Onset of Asian desertification by 22 Myr ago inferred from loess deposits in China, *Nature*, *416*, 159–163.

Hao, Q. Z., and Z. T. Guo (2004), Magnetostratigraphy of a late Miocene-Pliocene loess-soil sequence in the western Loess Plateau in China, *Geophys. Res. Lett.*, *31*, L09209, doi:10.1029/2003GL019392.

Hao, Q. Z., and Z. T. Guo (2005), Spatial variations of magnetic susceptibility of Chinese loess for the last 600 ka: Implications for monsoon evolution, *J. Geophys. Res.*, *110*, B12101, doi:10.1029/2005JB003765.

Heller, F., C. D. Shen, J. Beer, X. M. Liu, T. S. Liu, A. Bronger, M. Suter, and G. Bonani (1993), Quantitative estimates of pedogenic ferromagnetic mineral formation in Chinese loess and palaeoclimatic implications, *Earth Planet. Sci. Lett.*, *114*, 385–390.

Kirschvink, J. (1980), The least square line and the analysis of paleomagnetic data, *Geophys. J. R. Astron. Soc.*, *62*, 699–718.

Kukla, G. J., and Z. S. An (1989), Loess stratigraphy in central China, *Palaeogeogr. Palaeoclimatol. Palaeoecol.*, *72*, 203–225.

Li, F. J., N. Q. Wu, and D. Rousseau (2006), Preliminary study of mollusk fossils in the Qinan Miocene loess-soil sequence in western Chinese Loess Plateau, *Sci. Chin., Ser. D*, *49*, 724–730.

Liu, J. F., Z. T. Guo, Y. S. Qiao, Q. Z. Hao, and B. Y. Yuan (2006), Eolian origin of the Miocene loess-soil sequence at Qinan, China: Evidence of quartz morphology and quartz grain-size, *Chin. Sci. Bull.*, *51*(1), 117–120.

Liu, T. S. (1985), *Loess and the Environment*, 251 pp., China Ocean Press, Beijing.

Liu, T. S., and Z. T. Guo (1997), Geological environments in China and global change, in *Selected Works of Liu Tungsheng*, edited by A. S. An, pp. 192–202, Science Press, Beijing.

Lu, H. Y., X. Y. Wang, Z. S. An, X. D. Miao, H. B. Tan, R. X. Zhu, H. Z. Ma, Z. Li, and X. Y. Wang (2004), Geomorphologic evidence of phased uplift of the northeastern Qinghai-Tibet Plateau since 14 Million years ago, *Sci. Chin., Ser. D*, *47*, 822–833.

Qiao, Y. S., Z. T. Guo, Q. Z. Hao, Q. Z. Yin, B. Y. Yuan, and T. S. Liu (2006), Grain-size features of a Miocene loess-soil sequence at Qinan: Implications on its origin, *Sci. Chin., Ser. D*, *49*, 731–738.

Rea, D. K. (1994), The paleoclimatic record provided by eolian deposition in the deep sea: the geologic history of wind, *Rev. Geophys.*, *32*, 159–195.

Sun, D. H., X. H. Wu, and T. S. Liu (1996), Evolution of the summer monsoon regime over the Loess Plateau of the last 150 ka, *Sci. Chin., Ser. D*, *39*, 503–511.

Sun, X. J., and P. X. Wang (2005), How old is the Asian monsoon system? Palaeobotanical records form China, *Palaeogeogr. Palaeoclimatol. Palaeoecol.*, *222*, 181–222.

Zhou, L. P., F. Oldfield, A. G. Wintle, S. G. Robinson, and J. T. Wang (1990), Partly pedogenic origin of magnetic variations in Chinese loess, *Nature*, *346*, 737–739.

Ziegler, C. L., R. W. Murray, S. A. Hovan, and D. K. Rea (2007), Resolving eolian, volcanogenic, and authigenic components in pelagic sediment from the Pacific Ocean, *Earth Planet. Sci. Lett.*, *254*, 416–432.

Z. Guo and Q. Hao, Institute of Geology and Geophysics, Chinese Academy of Sciences, Beijing 100029, China. (ztguo@mail.iggcas.ac.cn)